

Grid Interactive Photovoltaic-Fuel Cell based Hybrid Generation System with Active and Reactive Power Control

Nilesh Shah* and Chudamani R**

In this paper, Photovoltaic (PV)-Fuel cell (FC) based grid interactive hybrid generation system is presented. The power generated by a PV system is highly dependent on weather condition. Hence, Fuel cell is used as back up source to supply the load demand along with PV under varying weather conditions. The PV-FC based hybrid generation system is developed using the model equations of PV and FC in the MATLAB/Simulink® environment. The PV-FC hybrid generation system is integrated with grid in two stages: dc-dc boost converter and three phase dc-ac inverter. Two separate dc-dc boost converters are used each with PV and FC system. In PV system, the dc-dc converter is used for Maximum Power Point (MPP) tracking and in FC system, the dc-dc converter is used for boosting the FC voltage. The MPP is tracked using fuzzy logic based controller under varying weather conditions. The power management algorithm proposed in this paper extracts and utilizes the maximum available power from PV array to supply the load demand. The FC is used to supply additional load demand higher than the maximum available PV power. The inverter injects the PV and FC power to load/grid in a controlled manner. The reference currents for current controller are generated using instantaneous power (p-q) theory. The hybrid generation system is tested under different load and weather conditions. The simulation results validate proposed power management algorithm for PV-FC based grid interactive hybrid generation system under varying environmental and load conditions.

Keywords: *Photovoltaic system, Fuel Cell, Hybrid Generation, Grid integration, Power Management, Active and Reactive Power Control, Maximum Power Point Tracking.*

1.0 INTRODUCTION

Recently, pollution of the environment and rising energy demand are the two major problems that challenge the mankind's existence. Consequently, the renewable energy sources are attracting more attention as alternate energy sources. Amongst various alternate energy sources, solar energy is gaining more popularity as it is available without any cost, produces no waste or pollution and has less geographical limitation compared to other renewable sources. Photovoltaic (PV) cell directly generates electricity from the light incident on it. Also, the installation of PV system is easy and as a result, the popularity of the PV system is increasing day by day [1].

To develop cleaner and efficient energy conversion device, recently Fuel Cell (FC) research and development have received a lot of attention due to their higher energy conversion efficiency and lower or non greenhouse-gas emissions than thermal engines in the process of converting fuel into usable energy [2].

The power generated by PV system is highly dependent on weather condition. Hence, hybridization of FC with PV form a very reliable distributed power generation where the FC acts as backup power solution during low PV output.

* Department of Electrical Engineering, Sarvajani College of Engineering & Technology (SCET), Surat, Gujarat, India Email: nilesh.shah@scet.ac.in

** Department of Electrical Engineering, Sardar Vallabhbhai National Institute of Technology (SVNIT), Surat, Gujarat, India Email: rc@eed.svnit.ac.in, drchudamani@gmail.com

In order to extract maximum power from PV array, it is required to operate at Maximum Power Point (MPP). Several techniques are presented for tracking MPP by researchers. In [3], comparison of various Maximum Power Point Tracking (MPPT) techniques like hill climbing method, incremental conductance method, open-circuit voltage and short-circuit current based technique, fuzzy logic control, neural network, ripple correlation method, current sweep and DC link capacitor droop control techniques are presented. These methods vary in complexity, convergence speed, performance and cost of the system.

Recently, fuzzy logic is becoming popular for tracking MPP due to its implementation simplicity, enhanced convergence speed and improved tracking performance with least oscillation. Several stand alone and grid connected PV systems use fuzzy logic controller for MPPT that takes at least two inputs and generate the control output [4-6]. The fuzzy logic based MPPT used in [7] control the duty ratio of the DC-DC converter in a stand-alone system using change in slope of P-V curve as input and change in voltage as output. A fuzzy logic based modified hill climbing method is proposed in [8] for MPP tracking in microgrid stand-alone PV system. The algorithm generates change in duty ratio as an output with change in power and change in current as input.

In this paper, the fuzzy logic based MPPT controller proposed in [9] by authors of this paper has been applied to a grid interactive PV-FC hybrid generation system. The proposed fuzzy logic based MPPT controller accepts single input that is slope of P-V curve (dP/dV) and generates the duty cycle for the boost converter as an output to operate the PV array at MPP and gives the maximum PV power to be injected into the grid. The proposed technique gives faster convergence with less complexity and gives least oscillations at MPP.

The authors in [2, 10] have introduced the system based on Proton Exchange Membrane Fuel Cell (PEMFC) technology that promises to make power more portable and convenient in a variety of applications. FC systems based on PEMFC

technology provide a more efficient and cleaner technology for the automotive industry.

The generalized steady-state electrochemical model of a PEMFC is presented in [11, 12]. It can be used for PEMFC of any active area and Nafion membrane thickness having capability of handling high current density. A simple and effective dynamic mathematical model of PEMFC is developed in [13] using MATLAB/Simulink through which the dynamic behavior of the PEMFC is analyzed. In [14], the fuel starvation phenomenon in PEMFC and its analysis is explained. In [15], the dynamic modeling, design, and simulation of a PEMFC and Ultracapacitor (UC) is developed using which FC and UC based energy source for stand-alone residential applications is developed.

A control strategy based on P-Q mode control and P-V mode control for the operation of the PEMFC based distributed generation system in grid connected and islanded mode is proposed in [16] for efficient power management of energy sources within the system. The authors in [17] presented modeling and control of a small scale grid-connected PEMFC system. The control strategy of the inverter is developed using $p-q$ theory.

In [18], modeling and control of PV/Fuel Cell/Battery hybrid power system that supports the local grid is presented. The inverter control strategy is based on d-q method for active and reactive power control. It is shown that the distributed generation system can be controlled to follow the local demand by allowing the grid to operate at nearly unity power factor.

The authors in [19] have developed FC based power supply system modeling for grid interfacing. The mathematical model is developed in per unit system using qd0 reference frame theory that define the real and reactive power flow limits, which can be supplied by the FC power plant. The system uses single stage PWM inverter as an interface between FC and grid.

The major objective of a hybrid generation system is to optimize the use of renewable power sources. In order to achieve this, proper power management system is required to be designed. In this paper, power management algorithm for grid interactive PV-FC based hybrid generation system is proposed and studied through simulation in MATLAB/Simulink. The major functional blocks of a PV-FC based hybrid generation system are PV array model, FC model, DC-DC converters, and 3 DC-AC converter which is used for grid integration.

A power management algorithm has been developed for the grid interactive PV-FC based hybrid generation system that feeds maximum available power from PV array and the deficit power is supplied by the FC. The control strategy of inverter for active as well as reactive power fed into the grid with power management between sources is developed using instantaneous power ($p-q$) theory [20, 21].

The proposed hybrid generation system improves the utilization of PV array and FC stack for different environment and load conditions. Apart from feeding active power generated by PV-FC sources using proposed power management system, the inverter control also incorporates the feature of reactive power compensation within the capacity of inverter rating.

Section-2 describes the configuration of grid interactive PV-FC based hybrid generation system along with modeling of various components and control strategy. The simulation results are discussed in section-3. Finally, concluding remarks are given in section-4.

2.0 GRID INTERACTIVE PV-FC BASED HYBRID GENERATION SYSTEM

The configuration of grid interactive PV-FC based hybrid generation system used for simulation study is shown in Figure 1. It consists of PV array, FC stack, DC-DC converters, voltage source inverter, MPPT controller, FC controller, inverter controller, ripple filter, grid and load.

The proposed system is designed to maximize the solar power utilization by operating PV array at MPP which minimizes the fuel demand. The duty ratio of boost converter used along with PV array is controlled using fuzzy logic based MPPT controller in order to inject maximum available power from the PV array to grid. The duty ratio of boost converter used along with FC is controlled to integrate the FC at DC link. The DC link voltage is maintained at 750 V by both the boost converters and the PI controller. The PI controller is required to regulate the DC link voltage specially when both PV and FC are not supplying power and the inverter is utilized for reactive power compensation. The inverter switching pulses are generated using hysteresis current controller.

2.1 PV SYSTEM MODELING

Photovoltaic is chosen as one of the renewable energy sources for hybrid generation system. In this section the modeling of various components of PV system is described. The electrical equivalent circuit model of PV cell consists of a current source in parallel with a diode [22, 23] as shown in Figure 2.

From the equivalent circuit of the PV cell shown in Figure 2, the PV cell output current (I_{cell}) is given by, where,

$$I_{cell} = I_{ph} - I_D - I_{sh} \quad \dots(1)$$

$$I_D = I_0 \left(e^{\frac{q(V_{cell} + I_{cell}R_S)}{kT}} - 1 \right) \quad \dots(2)$$

$$I_{sh} = \frac{V_{cell} + I_{cell}R_S}{R_{sk}} \quad \dots(3)$$

The parameters q , η , k and T denote the electronic charge (1.602×10^{-19} coulomb), ideality factor of the diode (1.2), Boltzmann constant (1.38×10^{-23}) and temperature in Kelvin respectively. I_{ph} is photocurrent, I_0 is diode reverse saturation current, I_{cell} and V_{cell} are the PV output current and voltage respectively.

As the value of R_{sh} is very large, it has a negligible effect on the I-V characteristics of PV cell or array. Thus (1) can be simplified to

$$I_{cell} = I_{ph} - I_0 \left(e^{\frac{q(V_{cell} + I_{cell}R_s)}{\eta kT}} - 1 \right) \quad \dots(4)$$

The simplified PV cell model is developed in MATLAB/SIMULINK™ environment using the model equations for the study of PV-FC based hybrid generation system. For grid interactive hybrid generation system, the PV array is designed using Solarex MSX60 PV modules. The parameters of the Solarex MSX60 PV module used for simulation 4

V_{PV} C_{PV} I_{La} I_{Lb} I_{Lc} I_{PV} I_{inva} I_{invb} I_{invc} Hysteresis Current Controller I_{refa} * I_{refc} * I_{sa} I_{sb} I_{sc} V_{sa} V_{sb} V_{sc} V_{PCC} V_{DC} DC-DC Boost Converter Reference Current Generation Using p-q theory V_{sc} CDC DC-AC Inverter I_{La} I_{Lb} I_{Lc} V_{sa} V_{sb} V_{sc} FUEL CELL DC-DC Boost Converter Ripple Filter MPPT Controller I_{PV} V_{PV} V_{DC} V_{FC} I_{FC} * P_{ref} P_{PV} P_{FC} V_{REF} V_{FC} 1 D_2 * V_{DC} V_{REF} PI P^* R_s L_s D_1 * P_{PV} P_{LOAD} P_{FC} * 1 V_{FC} If (Pload > Pinv) P_{FC} * = P_{FCmax} If (Pload < Pinv) P_{FC} * = Pload- P_{PV} I_{inva} I_{invb} I_{invc} PV ARRAY I_{refb} *

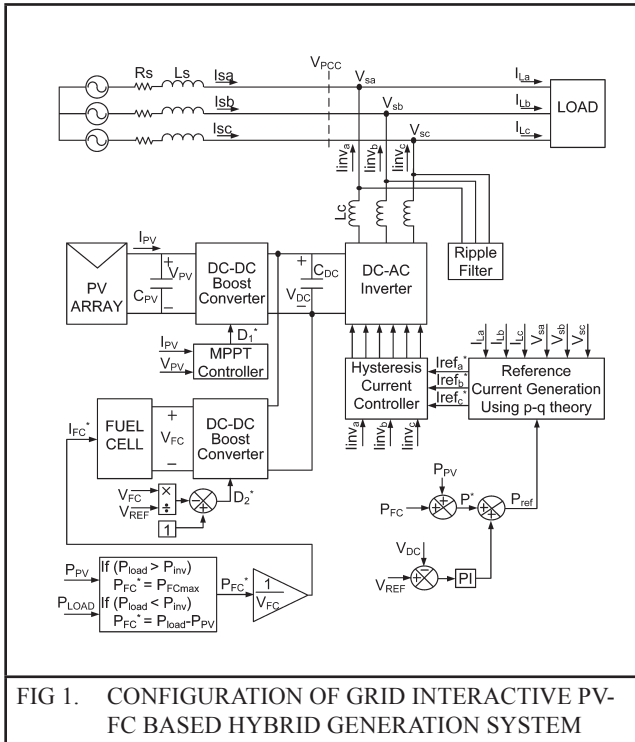


FIG 1. CONFIGURATION OF GRID INTERACTIVE PV-FC BASED HYBRID GENERATION SYSTEM

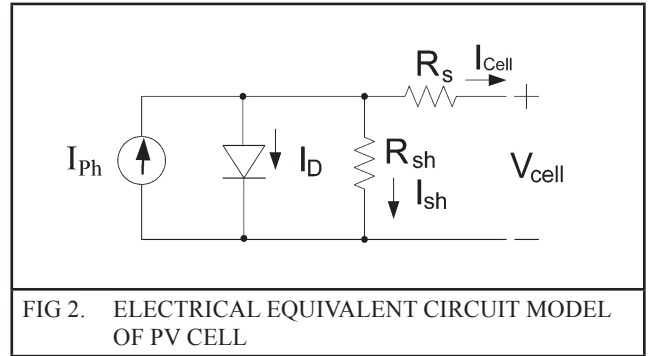


FIG 2. ELECTRICAL EQUIVALENT CIRCUIT MODEL OF PV CELL

study are shown in Table 1. The array is formed by connecting N_s series and N_p parallel connected PV modules as per required power. The current of PV array is given by,

$$I_{PV} = N_p \left\{ I_{ph} - I_0 \left(e^{\frac{q \left(\frac{V_{PV}}{N_s} + \frac{I_{PV} R_s}{N_p} \right)}{\eta kT}} - 1 \right) \right\} \quad \dots(5)$$

where in Eq. (5), V_{PV} and I_{PV} represents PV array output voltage and current respectively.

TABLE 1 SPECIFICATION OF SOLAREX MSX60 PV MODULE	
Parameter	Value
Short circuit current (A)	3.8
Open circuit voltage (V)	21.05
Voltage at MPP (V_{MPP}) (V)	17.1
Current at MPP (I_{MPP}) (A)	3.5
Maximum output power (W)	60
No. of cells in series	36
Reference Temperature	25°C
Reference solar insolation	1000 W/m ²

2.2 Maximum Power Point Tracking Controller

From the current-voltage (I-V) and power-voltage (P-V) characteristics of the PV module shown in Figure 3, it can be seen that the characteristics are highly nonlinear. Also, there exists single point on P-V curve where the PV can produce maximum power. The MPP changes with change in insolation and temperature. Therefore, an MPPT controller is required to extract maximum available power from the PV array under varying load and changing environmental conditions.

DC-DC boost converter is used as MPP tracker in two stage grid connected PV system. The output voltage of the boost converter depends on the duty cycle of the switching pulse that is controlled by the MPPT algorithm under varying environmental condition.

A fuzzy logic based MPPT controller proposed in [9] is used to extract maximum available power from PV array. The block diagram of the proposed Fuzzy Logic Controller (FLC) is shown in Figure 4. There are stages of the FLC: fuzzification, fuzzy rule base and defuzzification described as under:

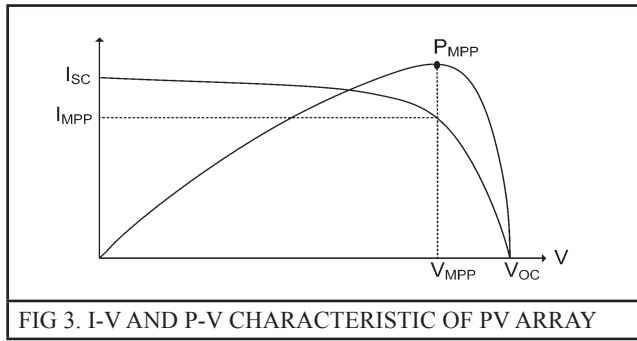


FIG 3. I-V AND P-V CHARACTERISTIC OF PV ARRAY

$$\Delta P(k) = P(k) - P(k - 1) \quad \dots(6)$$

$$\Delta V(k) = V(k) - V(k - 1) \quad \dots(7)$$

where P(k) and V(k) are the power and voltage of PV array at kth sampling instant, respectively.

Based on the magnitude of the slope of P-V curve, the proposed FLC divides the input and output into seven linguistic fuzzy sets: negative big (NB), negative medium (NM), negative small (NS), zero (ZO), positive big (PB), positive medium (PM) and positive small (PS). The membership functions of the input and output variables are shown in Figure 5 and Figure 6 respectively.

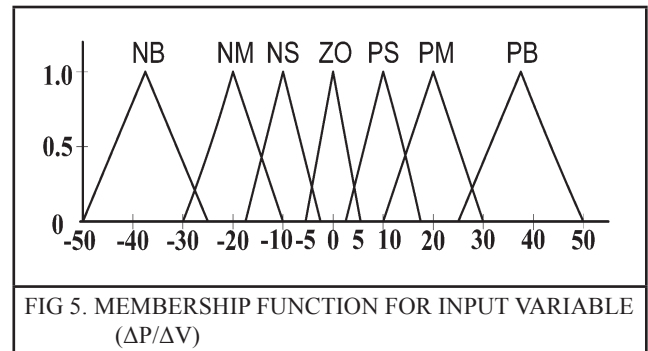


FIG 5. MEMBERSHIP FUNCTION FOR INPUT VARIABLE ($\Delta P/\Delta V$)

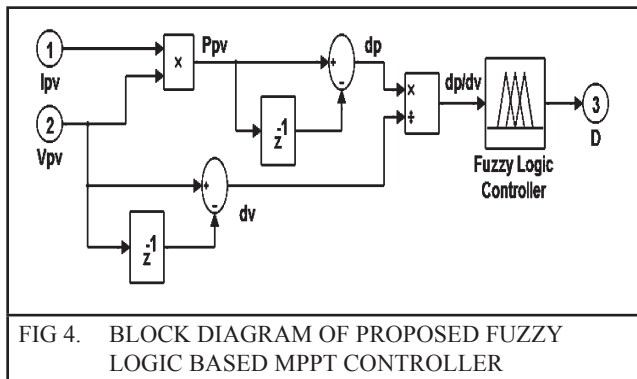


FIG 4. BLOCK DIAGRAM OF PROPOSED FUZZY LOGIC BASED MPPT CONTROLLER

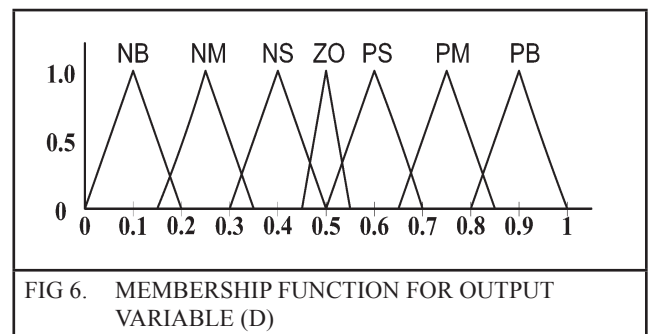


FIG 6. MEMBERSHIP FUNCTION FOR OUTPUT VARIABLE (D)

The first stage of FLC is fuzzification that divides the input and output into linguistic fuzzy sets from the prior knowledge of input and output range. The proposed FLC accepts single input that is the slope of the P-V curve $\Delta P(k)/\Delta V(k)$ and gives the duty ratio (D1*) as an output to generate the switching pulses for the boost converter in order to operate the PV array at MPP. The slope of P-V curve $\Delta P(k)/\Delta V(k)$ is determined by finding $\Delta P(k)$ and $\Delta V(k)$ after sampling the PV array voltage and current as follows:

The second stage of FLC precisely defines fuzzy rules in order to generate an output duty ratio D1 as per the magnitude of the slope of P-V curve in order to move the operating point towards MPP as per the logic specified as under:

$$\text{if } (\Delta P(k)/\Delta V(k) > 0)$$

D1 is decreased in order to increase the PV array operating voltage

$$\text{if } (\Delta P(k)/\Delta V(k) < 0)$$

D1 is increased in order to decrease the PV array operating voltage

The proposed technique uses seven rules for tracking the MPP as listed in Table 2.

TABLE 2							
FUZZY RULES							
$\Delta P / \Delta V$	NB	NM	NS	ZO	PS	PM	PB
D1	PB	PM	PS	ZO	NS	NM	NB

The third stage of FLC performs defuzzification to generate the single crisp value of output duty ratio D1 from the aggregated fuzzy set of output which includes a range of values. The centroid method [24] is used to convert the fuzzy subset of duty ratio D1 to a real number represented mathematically by,

$$z^* = \frac{\int \mu(z).zdz}{\int \mu(z)dz} \dots(8)$$

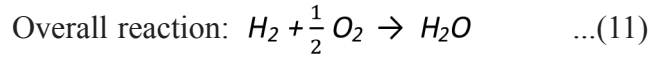
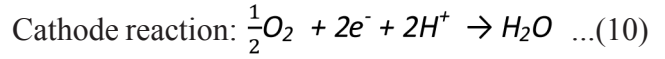
where, $z^* = D1^*$ which is the output of FLC that controls switching of boost converter, \int denotes algebraic integration and z is the aggregated fuzzy set of output.

2.3 Fuel Cell Modeling

Fuel cell is chosen as another renewable energy source for hybrid generation system due to its higher efficiency, scalability and lower pollution.

The PEMFC (Proton Exchange Membrane Fuel Cell) is used in PV-FC based hybrid generation system. It consists of a solid polymer electrolyte sandwiched between anode and cathode electrodes. Hydrogen (H2) is supplied to the anode where the H2 is oxidized and it will decompose in to H+ ions and electrons. The ions travel through the electrolyte and free electrons travel through the external circuit from the anode to the cathode which produces electricity because of a potential difference between them. At cathode, the Oxygen (O2) is reduced by consuming electrons from external circuit and water (H2O) is produced.

The overall electrochemical reactions in PEMFC at anode and cathode gas are as follows:



The mathematical model of PEMFC is used to establish a simple and effective dynamic PEMFC model through which the behavior of the transient voltage, power and efficiency of the PEMFC with changing load are analyzed. There exists a charge double layer in the fuel cell at the surface of the cathode that gives a simple equivalent circuit model of the PEMFC as shown in Figure 7. In this model, an electrical capacitor can be considered as the layer of charge on or near the electrode electrolyte interface, which is a store of electrical charge and energy [13].

R_a is the equivalent resistance that combines the R_{act} and R_{con} . The overall voltage drop V_d across R_a which is sum of voltage drop across R_{act} taking consideration of activation loss and voltage drop across R_{con} considering concentration loss is given by,

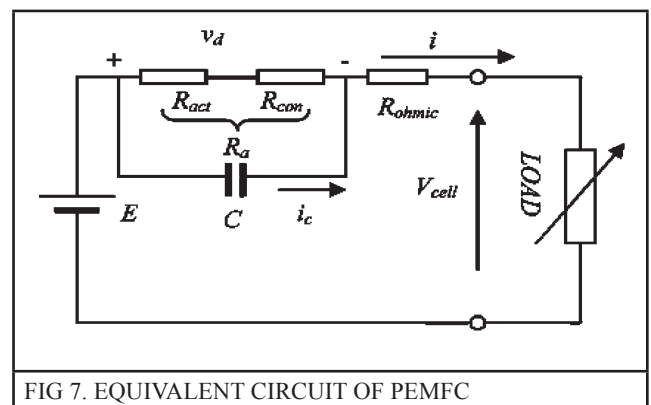


FIG 7. EQUIVALENT CIRCUIT OF PEMFC

$$V_d = (V_{act} + V_{con}) = i(R_{act} + R_{con}) \dots(12)$$

The dynamic characteristics of the single cell is expressed in the differential equation given by,

$$\frac{dv_d}{dt} = \frac{i}{C} - \frac{v_d}{\tau} \dots(13)$$

where,

$$\tau = \frac{C(V_{act}+V_{con})}{i-i_c} \dots(14)$$

The output voltage V_{cell} is defined as a function of cell current, reactant partial pressures, fuel cell temperature and membrane humidity [13, 15, 16]. The Nernst equation gives the ideal open circuit voltage between anode and cathode. In PEMFC, three types of losses occur; activation loss, ohmic loss and concentration loss that reduce the cell voltage at its terminal [13]. Considering these losses, the output voltage of PEMFC is given by,

$$V_{cell} = E_{Nernst} - V_{ohmic} - V_d \dots(15)$$

where E_{Nernst} is the thermodynamic potential and V_{ohmic} is the drop due to ohmic loss which is made up of two components, the voltage drop caused by the equivalent membrane impedance R_M and the voltage drop caused by the contact resistances R_c , given by,

$$V_{ohmic} = i_{Rohmic} = i (R_M + R_c) \dots(16)$$

$$E_{Nernst} = \frac{1}{2F} [\Delta G - \Delta S(T - T_{ref}) + RT \ln PH_2 + \ln PO_2] \dots(17)$$

where ΔG is Gibbs free energy change, ΔS is standard mole entropy change, F is Faraday's constant, R is gaseous constant, T_{ref} is the reference temperature and T is the actual temperature in Kelvin [13, 15].

By connecting N identical cells in series, the fuel cell stack is fabricated. The output voltage and the output power of the PEMFC stack is given by,

$$V_{FC} = NV_{cell} \dots(18)$$

$$\text{and } P_{FC} = V_{FC} I \dots(19)$$

The relationship between molar gas flows through the valve is proportional to its partial pressure [15-17] given by,

$$\frac{q_{H_2}}{P_{H_2}} = \frac{K_{an}}{\sqrt{M_{H_2}}} = K_{H_2} \dots(20)$$

$$\frac{q_{H_2O}}{P_{H_2O}} = \frac{K_{an}}{\sqrt{M_{H_2O}}} = K_{H_2O} \dots(21)$$

where,

- q_{H_2} : Molar flow of hydrogen
- q_{H_2O} : Molar flow of water
- P_{H_2} : Partial pressure of hydrogen
- P_{H_2O} : Partial pressure of water
- P_{O_2} : Partial pressure of oxygen
- K_{H_2} : Hydrogen valve molar constant
- M_{H_2} : Molar mass of hydrogen
- M_{H_2O} : Molar mass of water

For the hydrogen molar flow (kmol/s), there are three major factors such as the output flow, the input flow and the flow that takes part in the reaction [15-17]. These flows of hydrogen are represented by,

$$\frac{d}{dt} P_{H_2} = \frac{RT}{V_{an}} (q_{H_2}^{in} - q_{H_2}^{out} - q_{H_2}^r) \dots(22)$$

where V_{an} is the volume of anode (m^3).

The basic electrochemical relationship between the stack current and the molar flow of reacted hydrogen can be expressed [15-17] as

$$q_{H_2}^r = \frac{NI}{2F} = 2K_r I \dots(23)$$

where K_r is modeling constant [kmol/(s.A)].

Substituting Eq. (23) into (22), the hydrogen partial pressure can be written as,

$$\frac{d}{dt} P_{H_2} = \frac{RT}{V_{an}} (q_{H_2}^{in} - q_{H_2}^{out} - 2K_r I) \dots(24)$$

Using the equations derived for the PEMFC, a simulation model of PEMFC system is developed in Matlab/Simulink environment.

In order to meet the usage requirements, the basic target of the FC controller is to maintain optimal hydrogen utilization around 85%. Equation (23) shows that the reacting fuel is directly proportional

to the FC output current (I) [17]. Hence, the desired utilization is translated to a corresponding output current demand given by,

$$q_{H_2}^{in} = \frac{2K_r}{U_{f,opt}} I_{demand}$$

$$I_{demand} = \frac{U_{f,opt}}{2K_r} q_{H_2}^{in} \quad \dots(25)$$

where $U_{f, opt}$ is the optimal hydrogen utilization which is typically 80-90%.

The major task in using FC is to operate it at different power levels in hybrid generation system to optimally utilize power generated by different sources. In PV-FC hybrid generation system, the PV is operated at its MPP and under lower insolation conditions, the FC is utilized to supply the deficit power. Hence, in FC, the flow rates of H₂ and O₂ are required to be controlled which determine the overall control system of the FC. The current demand of the FC in terms of the load power demand is given by,

$$I_{demand} = P_{demand}/V_{FC} \quad \dots(26)$$

The current demand derived using (26) is given as input variable for controlling the FC stack in PV-FC based hybrid generation system. The H₂ and O₂ flow is controlled as per the current demand that produces FC stack voltage V_{FC} . The duty ratio of boost converter used along with FC is controlled by,

$$D_2^* = 1 - \frac{V_{REF}}{V_{FC}} \quad \dots(27)$$

where, V_{REF} is the reference DC link voltage that is regulated at 750 V in order to inject reactive power in addition to active power in the proposed grid interactive hybrid generation system.

2.4 Inverter Control Algorithm

The three phase voltage source inverter is used to integrate the PV array and FC system with the

grid. It injects the active and reactive power in a controlled manner under varying environment and load conditions.

The inverter switching pulses are generated using hysteresis current control technique [25]. The three phase reference currents for the hysteresis current controller are generated using the instantaneous power (p-q) theory [20, 21]. In order to inject active power generated by PV array and FC, the reference for active power (p^*) is generated according to (28). To provide reactive power compensation as per the load demand, the reference for reactive power (q^*) is generated according to (29) in which q_{filter} is the reactive power provided by ripple filter.

$$p^* = P_{PV} + P_{FC} \quad \dots(28)$$

$$q^* = q_{load} - q_{filter} \quad \dots(29)$$

The inverter switching losses are compensated by PV and FC when they supply active power and by the grid when PV and FC are unable to provide the required active power. The hysteresis current controller compares the three phase reference currents (I_{refa}^* , I_{refb}^* , I_{refc}^*) generated using p-q theory with the actual inverter currents (I_{inva} , I_{invb} , I_{invc}) and generates inverter switching pulses [24].

The ripple filter as shown in Figure 1 is a series R-C filter that absorbs the switching frequency ripples. The component values of ripple filters are so chosen as to absorb the high frequency components in multiple of switching frequency while maintaining the fundamental current drawn by ripple filter below 5% of the maximum load current. The ripple filter also provides reactive power compensation partially.

2.5 Proposed Power Management strategy for PV-FC based Hybrid Generation System

In the proposed grid interactive PV-FC based hybrid generation system, the PV array is operated at MPP using fuzzy logic based controller under varying insolation conditions. When PV output power is sufficient to supply the load demand

then the FC generator is kept OFF. During lower insolation conditions that may occur due to bad weather condition or during the day at evening, under which the PV power is insufficient to supply the load demand, the FC is controlled to supply the deficit load demand. Also, if the load demand is higher than the PV capacity, the FC is controlled to supply the increased load demand. The FC reference current is generated as per the difference between load power demand and PV generated power, using (26) and by controlling the fuel flow rate, the FC supplies the required difference power. During night or under zero insolation condition, the total load demand will be supplied by FC generator and grid. In a grid connected hybrid generation system, if PV and FC power are not sufficient, then the required power is drawn from the grid during day time as well as at night. When the system is very lightly loaded and the PV power is greater than the load demand, then the FC generator is switched OFF and the additional PV generated power is fed into the grid. The proposed grid interactive hybrid generation system is also utilized for reactive power compensation partially or fully within the inverter capacity under varying weather and load conditions especially during night and light load condition.

3.0 SIMULATION RESULTS

The proposed PV-FC based grid interactive hybrid generation system shown in Figure 1 is simulated using MATLAB/Simulink. The parameters of a 15.3 kW hybrid generation system used in the simulation study are shown in Table III.

The performance of the grid interactive PV-FC based hybrid generation system is analyzed for active and reactive power control under varying insolation and load conditions using proposed power management algorithm. While analyzing the performance, the PV array and FC maximum power rating is considered fixed as specified in Table III. Thus, maximum active power supplied by the inverter is $P_{max} = 15.3 \text{ kW}$ with $PPV_{max} = 10.8 \text{ kW}$ and $P_{FC_{max}} = 4.5 \text{ kW}$.

TABLE 3	
PARAMETERS OF PV-FC HYBRID GENERATION SYSTEM	
Description	Parameters
Grid voltage (L-L)	440 V
Grid frequency	50 Hz
Source Inductance	0.5 mH
DC link voltage	750 V
Interfacing Inductor	1.2 mH
Capacitor (DC bus side)	4000 μF
Capacitor (C _{pv})	2000 μF
No. of series connected PV modules	12
No. of parallel connected PV modules	15
PV array voltage at MPP	206.4 V
PV array current at MPP	52.5 A
PV array power at MPP	10.8 KW
No. of PEMFC stacks	250
Fuel Cell power	4.5 KW

The performance analysis is broadly divided into two test cases: (i) $P_{load} < P_{inv}$ and (ii) $P_{load} > P_{inv}$. When the load demand is less than the inverter capacity, the total load power is supplied by the inverter itself drawing no power from the grid. But when the load demand is greater than the inverter

capacity, the proposed energy management algorithm generates the references for the controller in such a way that the deficit power is drawn from the grid. These two cases are simulated for four different conditions of insolation and load variation and the results are presented. In all the conditions, the active power balance is given by,

$$P_{load} = P_{inv} + P_{grid} - P_{filter}$$

$$P_{load} = P_{pv} + P_{fc} + P_{grid} - P_{filter} \quad \dots(30)$$

where P_{filter} is the small amount of power loss that occur in ripple filter.

The reactive power balance under different insolation and load variations is given by,

$$Q_{load} = Q_{inv} + Q_{filter} \text{ with } Q_{grid} = 0 \quad \dots(31)$$

The current balance under different conditions of load and insolation variations is given by,

$$I_{load} = I_{inv} + I_{grid} \quad \dots(32)$$

It is also verified through the simulation results that under any situation of insolation and load variations, the grid current is in phase/anti-phase with the respective phase grid voltage that justifies almost full reactive power compensation by the inverter along with filter. It also justifies bidirectional power flow control in the grid interactive PV-FC based hybrid generation system using the proposed power management algorithm. The simulation results are presented for the following four conditions of insolation and load variations.

3.1 Performance under Constant Load with Fixed Insolation

The performance of the proposed PV-FC hybrid generation system for active and reactive power control with constant load under full insolation of 1000 W/m² is shown in Table 4. In case-(i), the load power demand is maintained at 7 kW and 3 kVAR respectively. As the load active power demand is less than the PV generated power under full insolation, the additional PV power is supplied to the grid. The power supplied by the FC in this case is zero. In case-(ii), the load active and reactive power demand is maintained at 19 kW and 8 kVAR respectively. For this case, the load active power demand is higher than the maximum capacity of the inverter and hence it is supplied by both the energy sources and deficit power is drawn from the grid.

From the results shown in Table IV, it can be noticed that active and reactive power balance follows (30) and (31) respectively.

TABLE 4										
PERFORMANCE FOR ACTIVE AND REACTIVE POWER CONTROL UNDER CONSTANT LOAD WITH FIXED INSOLATION										
Test Case	Insolation W/m ²	P _{grid} (kW)	P _{filter} (kW)	P _{inv} (kW)		P _{load} (kW)	Q _{grid} (kVAR)	Q _{filter} (kVAR)	Q _{inv} (kVAR)	Q _{load} (kVAR)
				P _{PV}	P _{FC}					
P _{load} < P _{inv}	1000	-3.56	0.040	10.6	0	7	0	0.6	2.4	3
P _{load} > P _{inv}	1000	3.94	0.040	10.6	4.5	19	0	0.6	7.2	8

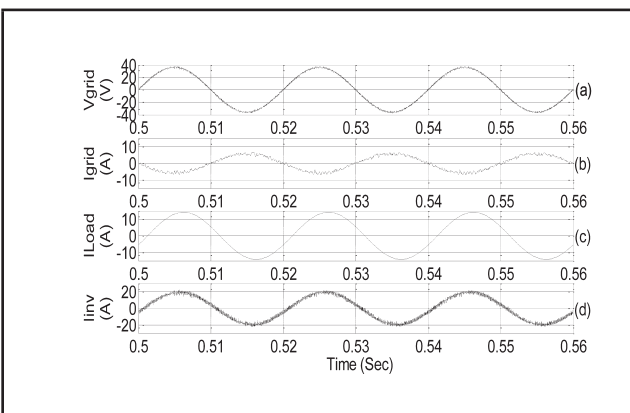


FIG 8. GRID VOLTAGE, GRID CURRENT, INVERTER CURRENT, LOAD CURRENT WITH CONSTANT LOAD AND INSOLATION (PLOAD < PINV)

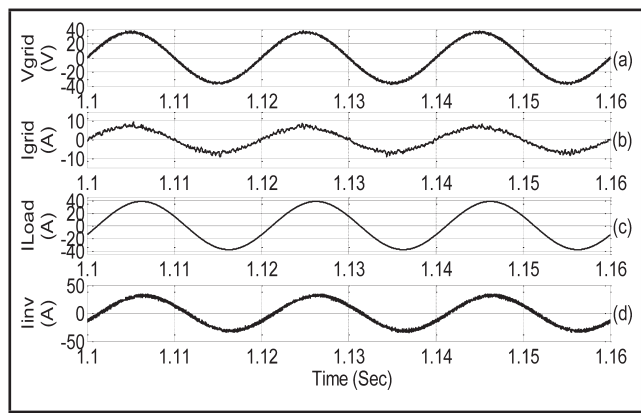


FIG 9. GRID VOLTAGE, GRID CURRENT, INVERTER CURRENT, LOAD CURRENT WITH CONSTANT LOAD AND INSOLATION (PLOAD > PINV)

The waveforms of phase-a grid voltage and the currents of grid, inverter and load for case-1 and case-2 are shown in Figure 8 and Figure 9 respectively. It can be seen from Figure 8(a) and 8(b) that the grid current is in anti-phase with the grid voltage that justifies that the current is injected into the grid as additional power is fed into the grid. It can be seen from Figure 9(a) and 9(b) that the grid current is in phase with the grid voltage that justifies that the current is drawn from the grid as load demand is higher than the inverter rating. The reactive power is almost fully compensated by the inverter and ripple filter. The current balance follows the relation given by (32).

3.2 Performance with step change in load under constant insolation of 1000W/m²

Figure 10 shows the active and reactive power balance and Figure 11 shows the corresponding phase-a current balance under varying load conditions at constant insolation of 1000 W/m².

During $0 \leq t \leq 1$ s, the load active power demand is 7 kW and reactive power demand is 3 kVAR i.e. $P_{load} < P_{inv}$. It can be seen in Figure 10(b) that the complete load demand is supplied by the PV array operating under full insolation. The power supplied by the FC is zero as seen in Figure 10(c) and as the PV generated power is higher than the load demand, the additional power is fed into the grid as shown in Figure 10(b) and Figure 10(d). It is even seen in Figure 11(b) that the grid current is in anti-phase with the grid voltage shown in Figure 11(a) indicating that the power is fed into the grid.

At $t = 1$ s, the load active and reactive power demand is suddenly increased from 7 kW to 19 kW and 3 kVAR to 8 kVAR respectively. In this case $P_{load} > P_{inv}$. Both PV array as well as FC operating together are unable to supply the increased load active power demand which is higher than the rating of the hybrid generation system. The PV array can supply only 10.8 kW power under full insolation. Hence, the FC is switched ON to meet the load demand. Since the load power demand is greater than the hybrid generation capacity, the FC will supply P_{FCmax}

and the deficit power is drawn from the grid which is seen in Figure 10(d).

It can be seen in Figure 10 (c) that under varying load condition, the reactive power drawn from grid is zero justifying almost full reactive power compensation by the inverter and ripple filter.

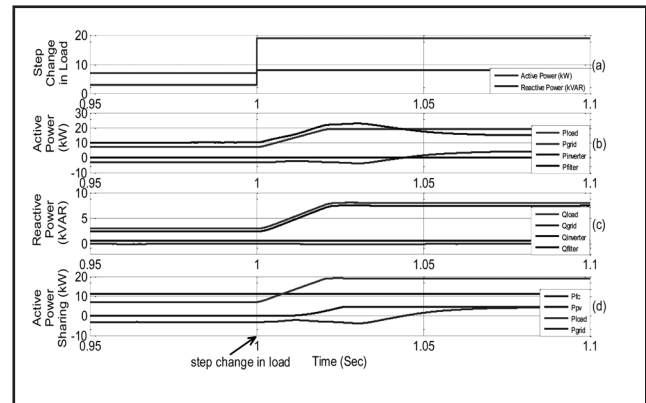


FIG 10. PERFORMANCE OF THE HYBRID GENERATION SYSTEM WITH INCREASE IN LOAD DEMAND UNDER CONSTANT INSOLATION

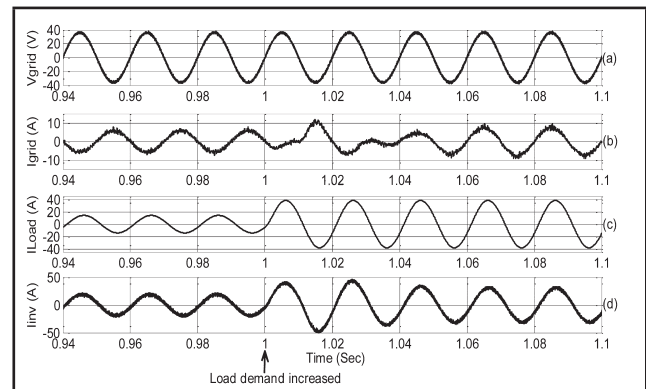


FIG. 11. GRID VOLTAGE, GRID CURRENT, LOAD CURRENT AND INVERTER CURRENT WITH INCREASE IN LOAD DEMAND UNDER CONSTANT INSOLATION

Figure 11 shows the waveforms of phase-a grid voltage and currents of the grid, load and inverter respectively. It is observed in Figure 11(b) that before $t = 1$ s, the grid current is in anti-phase with the grid voltage as inverter is supplying power into the grid and after $t = 1$ s, the grid current is in phase with the respective phase voltage indicating that the grid is supplying the increased load active power demand. This justifies the bidirectional power control capability of the hybrid generation system using proposed algorithm.

It is noticed in Figure 11(b) that the current drawn to/from the grid is nearly at unity power factor under varying load condition justifying reactive power compensation by the inverter. The current balance follows (32).

3.3 Performance under varying insolation condition at constant load

The performance of proposed hybrid generation system under varying solar insolation with constant load demand of 19 kW and 8 kVAR is shown in Figure 12 and Figure 13. The insolation is reduced from 1000 W/m² to 300 W/m² at t = 1 s as shown in Figure 12(a).

During $0 \leq t \leq 1$ s, the insolation level is full and hence the PV array is operating at its full rated capacity. At t=1 s, the insolation is reduced to 300 W/m², so the power generated by PV array also reduces. The constant load active power demand is greater than the rated capacity of the hybrid generation system and hence the FC supplies its rated power of 4.5 kW in addition to PV array and the deficit power is drawn from the grid as observed

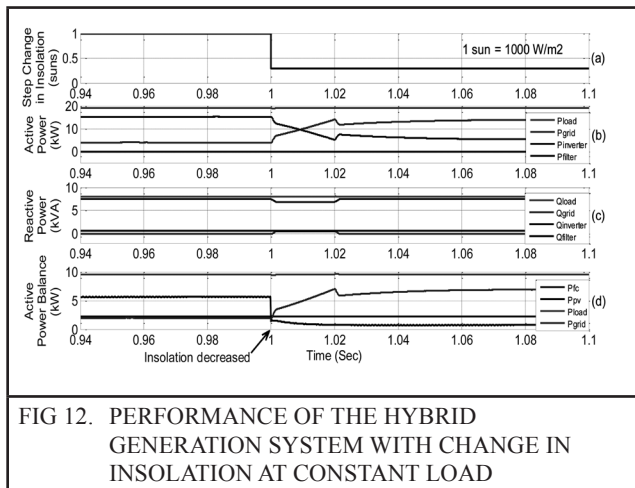


FIG 12. PERFORMANCE OF THE HYBRID GENERATION SYSTEM WITH CHANGE IN INSOLATION AT CONSTANT LOAD

in Figure 12(d). The reactive power is almost fully supplied by the inverter and ripple filter under varying insolation condition as seen in Figure 12(c).

Figure 13 shows the phase-a grid voltage and current waveforms of the grid, load, and inverter

respectively under varying insolation condition. The PV current reduces as the insolation is reduced at t = 1 s, and hence current supplied by the inverter To supply the constant load current, the current drawn from the grid increases as shown in Figure 13(b) and Figure 13 (c) respectively. Also the grid current is nearly in phase with the voltage ensuring reactive power compensation.

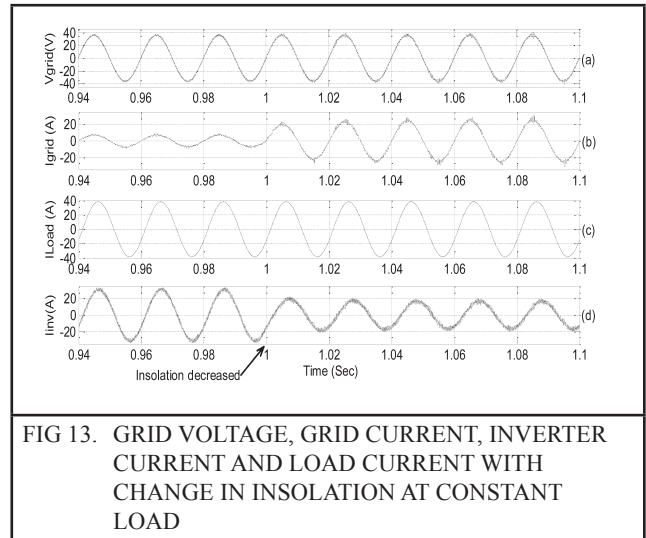


FIG 13. GRID VOLTAGE, GRID CURRENT, INVERTER CURRENT AND LOAD CURRENT WITH CHANGE IN INSOLATION AT CONSTANT LOAD

3.4 Performance under simultaneous change in both insolation and load

In this section, the proposed PV-FC based hybrid generation system is tested under worst case situation of reduction in insolation and increase in load demand simultaneously. The performance results are shown in Figure 14 and Figure 15. The solar insolation is reduced from 1000 W/m² to 300 W/m² at t=1 s as in Figure 14(a) and at the same instant the load active power demand is increased from 7 kW to 19 kW and load reactive power demand is increased from 3 kVAR to 8 kVAR as shown in Figure 14(b).

Before t = 1 s, the PV array is operating under full solar insolation of 1000 W/m². The load active power demand is less than the PV generated power and hence the additional PV power is supplied to the grid as seen in Figure 14(c) and Figure 14 (e). The power supplied by FC is zero as seen from Figure 14(e).

At $t = 1$ s, the insolation is reduced to 300 W/m² and load active and reactive power demand is increased to 19 kW and 8 kVAR respectively. Due to reduction in insolation as well as increase in load demand at $t=1$ s, both the sources are unable to supply the increased load active power demand and the deficit power is drawn from the grid as seen in Figure 14(c) and Figure 14(e). The reactive power is almost fully supplied by the inverter and ripple filter as seen in Figure 14(d).

Under the situation of reduction in insolation and increase in load demand simultaneously, the current balance waveforms are shown in Figure 15. It can be seen in Figure 15(b) that at $t=1$ s, the current drawn from the grid is increased in order to meet the increased load demand as the current supplied by inverter is reduced due to reduction in PV generated current as seen in Figure 15(c).

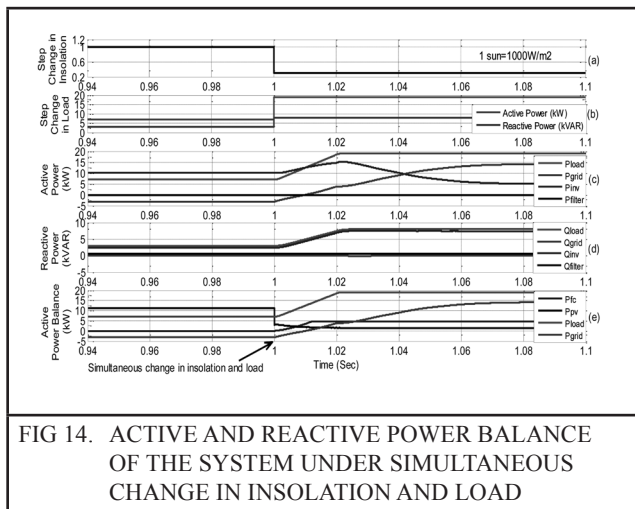


FIG 14. ACTIVE AND REACTIVE POWER BALANCE OF THE SYSTEM UNDER SIMULTANEOUS CHANGE IN INSOLATION AND LOAD

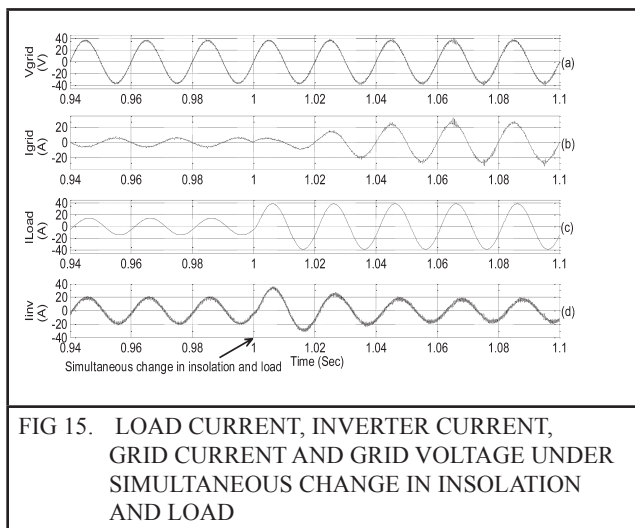


FIG 15. LOAD CURRENT, INVERTER CURRENT, GRID CURRENT AND GRID VOLTAGE UNDER SIMULTANEOUS CHANGE IN INSOLATION AND LOAD

From Figure 15(a) and Figure 15(b), it can be noticed that before $t = 1$ s, the grid current is in anti-phase with the grid voltage as inverter is supplying power into the grid and after $t = 1$ s, the grid current is in phase with the respective phase voltage indicating that active power is drawn from the grid.

4.0 CONCLUSIONS

In this paper, simulation study of PV-FC based grid interactive hybrid generation system is carried out using proposed power management algorithm. The proposed power management algorithm utilizes the PV generated power as per the available insolation and if PV power is insufficient to meet the load demand then the FC is controlled to supply the deficit load power. When the load demand is higher than the rating of both the renewable sources, the deficit power is drawn from the grid. Thus the proposed power management algorithm uses the energy sources optimally in the grid interactive hybrid generation system. The performance of the hybrid generation system is analyzed for active and reactive power control under varying insolation and load condition using fuzzy logic based MPPT algorithm and proposed power management strategy. The simulation results validate the robustness of the system using the proposed power management algorithm under varying load and weather conditions. The current fed into the grid is in phase/anti-phase with the grid voltage justifying reactive power compensation along with active power control.

REFERENCES

- [1] Alroza Khaligh, Omar G. Onar, "Energy Harvesting Solar, Wind, and Ocean Energy Conversion Systems", CRC Press, Taylor & Francis, 2010.
- [2] M. Farooque and H. C. Maru, "Fuel Cells- The Clean And Efficient Power Generators", Proc. of the IEEE on Engineering Our Future 1912-2012-2110 The Next Hundred Years, vol. 89, no. 12, pp. 1819-1829, December 2001.

- [3] T. Eswam and P. L. Chapman, "Comparison of Photovoltaic Array Maximum Power Point Tracking Techniques", *IEEE Trans. Energy Conv.*, vol. 22, no. 2, June 2007.
- [4] P. Takun, S. Kaitwanidvilai and C. Jettanasen, "Maximum Power Point Tracking using Fuzzy Logic Control for Photovoltaic Systems", *International conference of engineers and computer scientists (IMECS)*, Vol.-II, pp. 986-990, March-2011.
- [5] Carlos A. P. Tavares, Karla T. F. Leite, Walter I. Suemitsu, Maria D. Bellar, "Performance Evaluation of Photovoltaic Solar System with Different MPPT Methods", *Proc. of 35th Annual IEEE conference on Industrial Electronics (IECON'09)*, pp. 719-724, 2009.
- [6] Subiyanto, Azah Mohamed, and MA Hannan, "Hardware implementation of Fuzzy Logic based Maximum Power Point Tracking Controller for PV Systems", *Proc. of the 4th International Power Engineering and Optimization Conf. (PEOCO2010)*, pp. 435-439, June 2010.
- [7] Md. Asiful Islam, A. B. Talukdar, Nur Mohammad, P K Shadhu Khan, "Maximum Power Point Tracking of photovoltaic Arrays in Matlab Using Fuzzy Logic Controller", *Annual IEEE India conference (INDICON)*, 2010.
- [8] B. Alajmi, K. Ahmed, S. Finney, and B. Williams, "Fuzzy Logic Controlled Approach of a Modified Hill Climbing Method for Maximum Power Point in Microgrid Stand-alone Photovoltaic System", *IEEE Tran. Power Electronics*, Vol. 26, no. 4, pp. 1022-1030, April 2011.
- [9] N. Shah, R. Chudamani, "Grid Interactive PV System with Harmonic and Reactive Power Compensation Features using a Novel Fuzzy Logic Based MPPT", *Proc. of seventh international conference on Industrial and Information Systems (ICIIS 2012)*, August, 2012.
- [10] M. R. Nelson, Von Spakovsky, M. W. Ellis, "Fuel Cell Systems: Efficient, Flexible Energy Conversion For The 21st Century", *Proc. of the IEEE on An Energy ODYSSEY*, Vol. 89, no. 12, Dec. 2001.
- [11] J. Larminie and A. Dicks, "Fuel Cell Systems Explained", 2nd Edition, John Wiley & Sons Ltd, 2003.
- [12] R. F. Mann, J. C. Amphlett, Michael A.I. Hooper, H. M. Jensen, B. A. Peppley, P. R. Roberge, "Development and application of a generalized steady-state electrochemical model for a PEM fuel cell", *Science Direct Journal of Power Sources*, pp. 173-180, November 1999.
- [13] J. Jia, Q. Li, Y. Wang, W. T. Cham, And M. Han, "Modeling and Dynamic Characteristic Simulation of a Proton Exchange Membrane Fuel Cell", *IEEE Trans. Energy Conv.*, Vol. 24, no. 1, pp. 283-291, March 2009.
- [14] P. Thounthong, P. Sethakul, "Analysis of a Fuel Starvation Phenomenon of a PEM Fuel Cell", *Proc. of IEEE Power Conversion Conference (PCC '07)*, Nagoya. pp. 731 - 738, April 2007.
- [15] M. Uzunoglu, and M. S. Alam, "Dynamic Modeling, Design, and Simulation of a Combined PEM Fuel Cell and Ultracapacitor System for Stand-Alone Residential Applications", *IEEE Trans. Energy Conv.*, Vol. 21, No. 3, pp. 767-775, September 2006.
- [16] A. A. Salam, A. Mohamed, M. A. Hannan, H. Shareef, "A 50KW PEM fuel cell Inverter-Based Distributed Generation System for Grid Connected and Islanding Operation", *Proc. of IEEE Region 10 conference-TENCON 2009*, pp. 1-5, Jan. 2009.
- [17] D. Georgakis, S. Papathanassiou and S. Manias, "Modeling and control of a small scale grid-connected PEM fuel cell system" *Proc. of IEEE 36th Power Electronics Specialists Conference*, pp. 1614-1620, June 2005.
- [18] M. Samiei Moghaddam, A. Hajizadeh, "Control of Hybrid PV/Fuel Cell/Battery Power Systems", *Proc. of Power Electronics*,

- Drives And Energy Systems (PEDES) & 2010 Power India Joint International Conference, pp. 1–7, 20-23 Dec. 2010.
- [19] S. Jain, J. Jiang, X. Huang, and S. Stevandic, “Modeling of Fuel Cell Based Power Supply System for Grid Interface”, *IEEE Trans. Ind. Appl.*, vol. 48, pp. 1142 – 1153, 2012.
- [20] H. Akagi, E. H. Watanabe and M. Aredes, “Instantaneous Power Theories & Application to Power Conditioning”, John Willey Publication, pp. 110-180, 2007.
- [21] H. Akagi, Y. Kanazawa, and A. Nabae, “Instantaneous Reactive Power Compensators Comprising Switching Devices without Energy Storage Components”, *IEEE Trans. Ind. Appl.*, Vol. IA-20, no. 3, May/June 1984.
- [22] Chetan Singh Solanki, “Solar Photovoltaics: Fundamentals, Technologies and Applications”, PHI Learning PVT. LTD., New Delhi, 2009.
- [23] G. Walker, “Evaluating MPPT converter topologies using a Matlab PV model”, *Journal of Electrical and Electronics Engg.*, Australia, Vol. 21, pp. 49-55, 2001.
- [24] Timothy J. Ross, “Fuzzy Logic with Engineering Applications”, Mcgraw-Hill International Edition, 1997.
- [25] B. K. Bose, “Modern Power Electronics and AC Drives”, Prentice Hall PTR, pp. 236-239, 2002.

